Inorg. Chem. **2008**, *47*, 11257−11268

Second-Order Self-Organization in Coordination-Driven Self-Assembly: Exploring the Limits of Self-Selection

Brian H. Northrop,*,† Hai-Bo Yang,*,‡ and Peter J. Stang†

University of Utah, Department of Chemistry, 315 South 1400 E, Salt Lake City, Utah 84112, and Shanghai Key Laboratory of Green Chemistry and Chemical Processes, Department of Chemistry, East China Normal University, Shanghai 200062, China

Received September 5, 2008

Self-organization during the self-assembly of a series of functionalized bispyridyl organic donors with complementary di-Pt(II) acceptors into supramolecular rhomboids and rectangles is explored. The connectivity and location of functional groups on the organic donors ensures that they do not interfere sterically or electronically with their respective binding sites. Carefully controlled reaction conditions are employed so that the only means of self-organization during self-assembly is through "second-order" effects arising from the distal functional groups themselves. With the selection of functionalized systems studied, the extent of second-order self-organization varies from essentially zero to quite pronounced.

Introduction

Self-assembly[1] and self-organization[2] are related concepts that account for much of the beauty and complexity of the natural world across all length scales. Beginning with seminal studies of molecular recognition in the 1960s and 1970s by Pedersen, Lehn, Sauvage, Dietrich, Cram, and others,[3] chemists have developed a variety of means of using noncovelant interactions—hydrogen bonding, charge−charge, donor−acceptor, metal−ligand coordination, etc.—to drive the self-assembly of predesigned molecules into particular shapes and topologies. While it may not always be possible to predict *a priori* the exact shapes or constitutions of supramolecular assemblies, it is often possible and desirable to limit the range of potential assemblies by using relatively few, specifically designed complimentary pairs of component molecules: one hydrogen bond donor and one hydrogen bond acceptor, one π-electron-rich donor and one π-electron-poor acceptor, a metal with one free Lewis acidic site and a ligand with one free Lewis basic site, etc. Much more complicated systems and situations arise when multiple components are combined into one complex mixture. The presence of many species in one mixture, whether their self-assembly protocols are independent (orthogonal) or competitive (communicative), presents a situation wherein self-organization becomes a possibility.

Self-organization is the process where complimentary components of a multicomponent mixture selectively recognize each other to form well-defined assemblies of discrete structures at the expense of a random, statistical mixture of products. Such "order out of chaos" self-organization processes are present throughout nature, from the formation of galaxies to weather patterns to biological systems.[4] Proteins, for example, are able to perform incredibly complex and specific functions throughout the body, perhaps the ultimate complex mixture, alongside other proteins performing entirely different tasks. These diverse functions are largely carried out simultaneously despite the fact that all proteins

* To whom correspondence should be addressed. E-mail: b.northrop@utah.edu (B.H.N), yanghb76@yahoo.com.cn (H.-B.Y.).
† University of Utah.
‡ East Shanghai Normal University.

(1) (a) Lehn, J.-M. *Angew. Chem., Int. Ed. Engl.* **1990**, *29*, 1304. (b) Lindsey, J. S. *New. J. Chem.* **1991**, *15*, 153. (c) Philp, D.; Stoddart, J. F. *Angew. Chem., Int. Ed. Engl.* **1996**, *35*, 1154. (d) Rebek, J., Jr *Acc. Chem. Res.* **1999**, *32*, 278. (e) Yaghi, O. M.; O'Keeffe, M.; Ockwig, N. W.; Chae, H. K.; Eddaoudi, M.; Kim, J. *Nature* **2003**, *423*, 705.

(2) (a) Orr, G. W.; Barbour, L. T.; Atwood, J. L. *Science* **1999**, *285*, 1049. (b) Storhoff, J. J.; Mirkin, C. A. *Chem. Rev.* **1999**, *99*, 1849. (c) Lehn, J.-M. *Science* **2002**, *295*, 2400. (d) Lehn, J.-M. *Proc. Natl. Acad. Sci. U.S.A.* **2002**, *99*, 4763. (e) Lehn, J.-M. *Rep. Prog. Phys.* **2004**, *67*, 249. (f) Hollingsworth, M. D. *Science* **2002**, *295*, 2410.

(3) (a) Deitrich, B.; Lehn, J.-M.; Sauvage, J. P. *Tetrahedron Lett.* **1969**, *34*, 2889. (b) Pederson, C. J. Ger. Offen, Application: DE 70-2015732, 1970. (c) Lehn, J.-M.; Sauvage, J. P.; Dietrich, B. *J. Am. Chem. Soc.* **1970**, *92*, 2916. (d) Cram, D. J.; Cram, J. M. *Acc. Chem. Res.* **1978**, *11*, 8. (e) Lehn, J.-M. *Acc. Chem. Res.* **1978**, *11*, 49. (f) Pederson, C. J.; Lehn, J.-M.; Cram, D. J. *Resonance* **2001**, *6*, 71.

(4) (a) Gleick, J. *Chaos: Making a New Science*. Penguin: New York, 1988. (b) Kauffman, S. *At Home in the Universe*; Oxford University Press: Oxford, U.K., 1995.

10.1021/ic801711q CCC: $40.75
Published on Web 11/04/2008

are built from collections of the same 20 amino acid building blocks. No system, however, is truly perfect, and it is possible, even necessary at times, to disrupt this elegant self-organization such as through the introduction of pharmaceuticals into the body. Recently, chemists have explored the concepts of self-organization in purely synthetic systems. Initial studies by Lehn,[5] Schneider,[6] and Raymond[7] involving the transition metal mediated self-organization of helices demonstrated how the information encoded within specific building blocks can govern the exclusive assembly of multiple, discrete homohelical constructs from within a complex mixture and without any evidence of heterohelical assemblies.

More recently, a number of studies have shown that self-organization in synthetic systems is not always exclusively self-selective and is often more statistical. Stack[8] and Davis[9] have both studied chiral self-organization and have found examples where exclusively homochiral assemblies form when cations (Cu^{II} or Ba^{II}) are added to racemic mixtures of diiminopyridine ligands or a guanosine-quartet precursor, respectively. Slight modifications of either the precursors or cations, however, result in mixtures of homochiral and heterochiral assemblies, though a preference for homochiral assemblies was observed in each case. Lehn,[10] Raymond,[11] Nitschke,[12] Severin,[13] Barboiu,[14] and Isaacs[15] have performed similar investigations of the effects that size, geometry, concentration, and "external effectors" (e.g., cations of different charge or metals with varying coordination number/geometry) have on the extent of self-organization. These studies have found that a range of potential outcomes, from statistical dynamic combinatorial libraries to exclusive "narcissistic" self-organization,[16] can be observed. Isaacs[15a] has recently posed the question of whether self-organization in designer systems should be expected or surprising; is it the "exception or the rule?" By investigating the simultaneous self-assembly of nine components in the presence of barium picrate Isaacs observed near-exclusive self-organization of eight[17] supramolecules and, after thoroughly investigating the effects of different conditions, determined that only small differences in equilibrium constant (<10-fold) are necessary to promote such discriminating results. It was noted, however, that the variety of complimentary components were chosen to fit criteria that were deemed sufficient for exclusive self-organization and a number of conditions were noted when such exclusivity would likely not be observed, ultimately concluding that self-organization should neither be expected nor surprising. These collective observations suggest that there is a self-organization "spectrum" from statistical (no organization) to exclusive (organization of either pure homo- or pure heteroassemblies) and that where a mixture falls on that spectrum depends upon size, shape, geometry, concentration, k_{eq}, and various external effectors.

We have previously explored[18−21] the concept of self-organization during the self-assembly of square-planar Pt(II) acceptors and pyridyl donors into supramolecular polygons and polyhedra. For example, mixing a single ditopic 4,4′-bipyridine donor with three different di-Pt(II) acceptors of varying geometries (0°, 60°, and 90°) resulted in the exclusive formation of discrete assemblies of supramolecular rectangles, triangles, and squares, respectively, from within the complex mixture.[18] Extending these studies into the third dimension, mixtures of two different tritopic donors with one ditopic acceptor or, alternatively, one tritopic donor with two ditopic acceptors resulted, in each case, in the exclusive formation of discrete M_3L_2 polyhedra.[19] Size-selective self-sorting has also been observed during the self-assembly of 2D metallacycles when linear ditopic bispyridyl donors of different length were combined with 0° or 60° di-Pt(II) acceptors.[20] In both cases, only those metallacycles with identical length bispyridyl donors were found, and no mixed donor assemblies were observed. Recently, we have examined the self-organization of supramolecular squares composed of a 90° di-Pt(II) acceptor and asymmetric (4-ethynylpyridyl)-substituted pyridine donors, with the substituents being -CH_3 or -Cl groups located at the α or β position(s).[21] With such asymmetric ligands, we were able to study the

(5) (a) Krämer, R.; Lehn, J.-M.; Marquis-Rigault, A. *Proc. Natl. Acad. Sci. U.S.A.* **1993**, *90*, 5394. (b) Smith, V.; Lehn, J.-M. *Chem. Commun.* **1996**, 2733. (c) Funeriu, D. P.; Lehn, J.-M.; Fromm, K. M.; Fenske, D. *Chem.—Eur. J.* **2000**, *6*, 2103.

(6) (a) Albrecht, M.; Schneider, M.; Röttele, H. *Angew. Chem., Int. Ed.* **1999**, *38*, 557. (b) Albrecht, M.; Schneider, M. *Eur. J. Inorg. Chem.* **2002**, 1301.

(7) (a) Caulder, D. L.; Raymond, K. N. *Angew. Chem., Int. Ed. Engl.* **1997**, *36*, 1440. (b) Ziegler, M.; Miranda, J. J.; Anderson, U. N.; Johnson, D. W.; Leary, J. A.; Raymond, K. N. *Angew. Chem., Int. Ed.* **2001**, *40*, 733.

(8) Masood, M. A.; Enemark, E. J.; Stack, T. D. P. *Angew. Chem., Int. Ed.* **1998**, *37*, 928.

(9) Shi, X.; Fettinger, J. C.; Davis, J. T. *J. Am. Chem. Soc.* **2001**, *123*, 6738.

(10) (a) Giuseppone, N; Schmitt, J.-L.; Lehn, J.-M. *Angew. Chem., Int. Ed.* **2004**, *43*, 4902. (b) Giuseppone, N.; Lehn, J.-M. *J. Am. Chem. Soc.* **2004**, *126*, 11448. (c) Giuseppone, N.; Fuks, G.; Lehn, J.-M. *Chem.—Eur. J.* **2006**, *12*, 1723.

(11) (a) Caulder, D. L.; Powers, R. E.; Parac, T. N.; Raymond, K. N. *Angew. Chem., Int. Ed.* **1998**, *37*, 1840. (b) Bruckner, C.; Powers, R. E.; Raymond, K. N. *Angew. Chem., Int. Ed.* **1998**, *37*, 1837.

(12) (a) Schultz, D.; Nitschke, J. R. *Proc. Natl. Acad. Sci. U.S.A.* **2005**, *102*, 11191. (b) Schultz, D.; Nitschke, J. R. *Angew. Chem., Int. Ed.* **2006**, *45*, 2453. (c) Hutin, M.; Frantz, R.; Nitschke, J. R. *Chem.—Eur. J.* **2006**, *12*, 4077. (d) Nitschke, J. R. *Acc. Chem. Res.* **2007**, *40*, 103.

(13) (a) Severin, K. *Chem.—Eur. J.* **2004**, *10*, 2565. (b) Saur, I.; Severin, K. *Chem. Commun.* **2005**, 1471. (c) Saur, I.; Scopelliti, R.; Severin, K. *Chem.—Eur. J.* **2006**, *12*, 1058.

(14) (a) Barboiu, M.; Petit, E.; Vaughan, G. *Chem.—Eur. J.* **2004**, *10*, 2263. (b) Dumitru, F.; Petit, E.; van der Lee, A.; Barboiu, M. *Eur. J. Inorg. Chem.* **2005**, 4255. (c) Barboiu, M.; Petit, E.; van der Lee, A.; Vaughan, G. *Inorg. Chem.* **2005**, *44*, 5649. (d) Legrand, Y.-M.; van der Lee, A.; Barboiu, M. *Inorg. Chem.* **2007**, *46*, 9540.

(15) (a) Wu, A.; Isaacs, L. *J. Am. Chem. Soc.* **2003**, *125*, 4831. (b) Mukhopadhyay, P.; Wu, A.; Isaacs, L. *J. Org. Chem.* **2004**, *69*, 6157. (c) Lui, S.-M.; Ruspic, C.; Mukhopadhyay, P.; Chakrabarti, S.; Zavalij, P.; Isaacs, L. *J. Am. Chem. Soc.* **2005**, *127*, 15959. (d) Mukhopadhyay, P.; Zavalij, P. Y.; Isaacs, L. *J. Am. Chem. Soc.* **2006**, *128*, 14903.

(16) Taylor, P. N.; Anderson, H. L. *J. Am. Chem. Soc.* **1999**, *121*, 11538.

(17) While the simultaneous self-assembly of nine components was studied, only eight supramolecules were obtained because two of the nine components were complementary constituents that self-assemble to form one single supramolecule.

(18) Addicott, C.; Das, N.; Stang, P. J. *Inorg. Chem.* **2004**, *43*, 5335.

(19) Yang, H.-B.; Ghosh, K.; Northrop, B. H.; Stang, P. J. *Org. Lett.* **2007**, *9*, 1561.

(20) Zheng, Y.-R.; Yang, H.-B.; Northrop, B. H.; Ghosh, K.; Stang, P. J. *Inorg. Chem.* **2008**, *47*, 4706.

(21) Zhao, L.; Northrop, B. H.; Zheng, Y.-R.; Yang, H.-B.; Lee, H. J.; Lee, Y. M.; Park, J. Y.; Chi, K.-W.; Stang, P. J. *J. Org. Chem.* **2008**, *73*, 6580–6586.

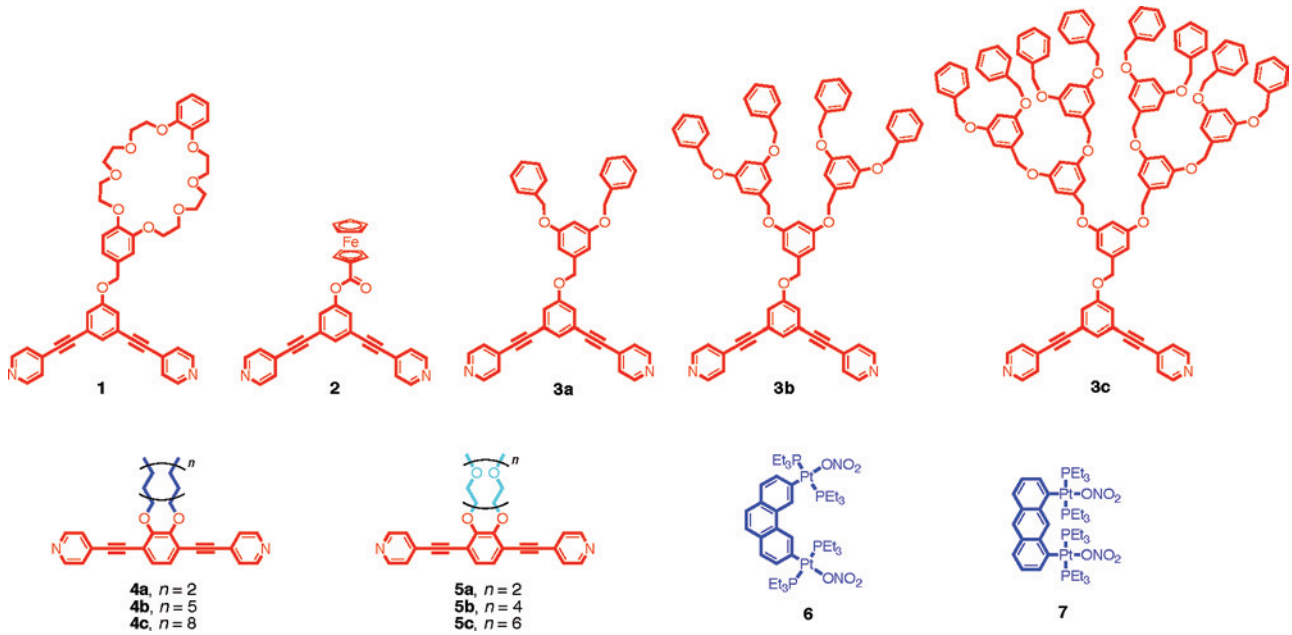

Figure 1. Chemical structures of **DB24C8**-functionalized 120° bispyridyl donor **1**, ferrocenyl-functionalized 120° donor **2**, dendronized 120° donors **3a**−**c**, hydrophobic 180° donors **4a**−**c**, and hydrophilic 180° donors **5a**−**c**, as well as 60° and 0° di-Pt(II) acceptors **6** and **7**.

effects of steric interactions on self-organization processes. It was observed that as steric bulk around the pyridyl donor nitrogen atom increased the extent of self-organization increased as well.

These studies reflect, to the best of our knowledge, the only reported examples of self-organization involving square platinum−pyridine complexes, which have proven to be especially versatile and powerful in molecular self-assembly. Across these four studies, the only variables investigated have been the effects of geometry, dimensionality, size, and sterics on the self-organization of Pt(II)−pyridine-based metallacycles and metallacages, while the concentration, temperature, the oxidation state and coordination number of the metal, and k_{eq} were kept constant and no external effectors were introduced into the systems. Though important, these studies leave the door open for further investigations wherein the size, geometry, dimensionality, and sterics around the coordination site of all building blocks are kept constant. Such studies, in which all variables that have been heretofore considered contributory to self-organization are kept constant, allow for the influence of purely second-order effects to be investigated, further exploring the limits of self-organization. In this Article, we report the effects of second-order interactions, those far removed from the principle determinants/directors of molecular self-assembly processes, on the self-organization of supramolecular rhomboids and rectangles and show that these secondary effects can, but do not always, play a role in self-organization processes.

Results and Discussion

We have recently reported the synthesis of a series of functionalized 120° and 180° ditopic bispyridyl donors (Figure 1). Three different types of functionalized 120° donors were prepared by covalently attaching a dibenzo[24]crown-8 (**DB24C8**) derivative,[22] a redox-active ferrocene derivative,[23] or a Fréchet-type dendritic derivative[24] to a 3,5-bis(4-ethynylpyridyl)-phenol. A series of 180° donors bearing C_6H_{13}, $C_{12}H_{25}$, and $C_{18}H_{37}$ straight chain hydrophobic functionalities (C_6, C_{12}, and C_{18}) or methylated di-, tetra-, and hexaethyleneglycol hydrophilic functionalities (DEG, TEG, and HEG) has also been prepared.[25] The placement of **DB24C8**, ferrocenyl, dendritic, and hydrophobic/hydrophilic functionalities onto their respective 120° and 180° donors was chosen to be sufficiently far from donor binding sites that they do not interfere structurally (sterically) or electronically with their pyridyl donor moieties and their ability to undergo self-assembly with complementary di-Pt(II) acceptors would not be compromised. Indeed, when mixed with a 60° di-Pt(II) acceptor, the functionalized 120° donors self-assemble into bisfunctionalized rhomboids,[22b,23a,24b] and when mixed with a molecular "clip", the 180° donors form hydrophobic and hydrophilic rectangles,[25] all in essentially quantitative isolated yields (>95%). Upon the successful self-assembly of functionalized metallacyclic rhomboids and rectangles, the possibility of "mixed-functionality" metallacycles and the prospect of self-organization became of immediate interest. Furthermore, the range of different donor

(22) (a) Yang, H.-B.; Ghosh, K.; Northrop, B. H.; Zheng, Y.-R.; Lyndon, M. M.; Muddiman, D. C.; Stang, P. J. *J. Am. Chem. Soc.* **2007**, *129*, 14187. (b) Ghosh, K.; Yang, H.-B.; Northrop, B. H.; Lyndon, M. M.; Zheng, Y.-R.; Muddiman, D. C.; Stang, P. J. *J. Am. Chem. Soc.* **2008**, *130*, 5320.

(23) (a) Yang, H.-B.; Ghosh, K.; Zhao, Y.; Northrop, B. H.; Lyndon, M. M.; Muddiman, D. C.; White, H. S.; Stang, P. J. *J. Am. Chem. Soc.* **2008**, *130*, 839. (b) Ghosh, K.; Zhao, Y.; Yang, H.-B.; Northrop, B. H.; White, H. S.; Stang, P. J. *J. Org. Chem.*, published online October 8, **2008**, DOI: 10.1021/jo801692y.

(24) (a) Yang, H.-B.; Das, N.; Huang, F.; Hawkridge, A. M.; Muddiman, D. C.; Stang, P. J. *J. Am. Chem. Soc.* **2006**, *128*, 10014. (b) Yang, H.-B.; Hawkridge, A. M.; Huang, S. D.; Das, N.; Bunge, S. D.; Muddiman, D. C.; Stang, P. J. *J. Am. Chem. Soc.* **2007**, *129*, 2120.

(25) Northrop, B. H.; Glöckner, A.; Stang, P. J. *J. Org. Chem.* **2008**, *73*, 1787.

Scheme 1. Potential Second-Order Self-Organization Effects Are Investigated through the Self-Assembly of (A) Unrelated **DB24C8** and Ferrocene Functionalized Bispyridyl Donors **1** and **2** with 60° Di-Pt(II) Acceptor **6**, (B) Related though Different Generation Dendronized 120° Bispyridyl Donors **3a** and **3b** (or **3b** and **3c**) with 60° Di-Pt(II) Acceptor **6**, and (C) Like-Sized Hydrophobic (**4a**−**c**) and Hydrophilic (**5a**−**c**) 180° Bispyridyl Donors with a 0° Di-Pt(II) Molecular Clip[a]

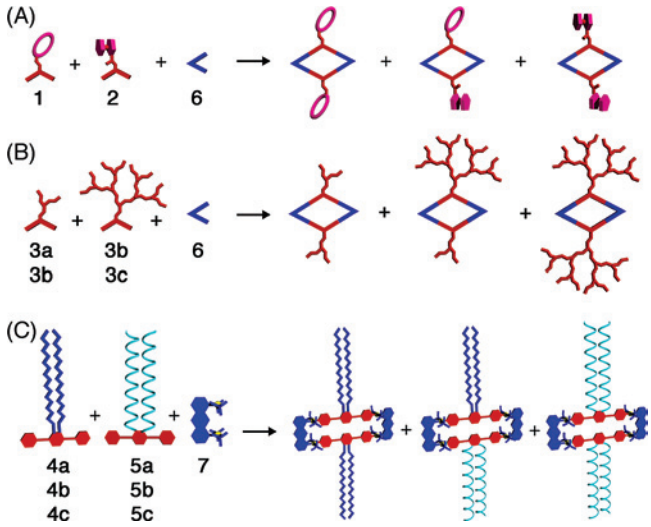

[a] In each case the donor/donor/acceptor ratio is 1:1:2.

functional groups allows for a variety of different potential second-order self-organization effects to be studied: mixtures of unrelated functionalities (**DB24C8**/ferrocenyl), structurally related moieties that vary in size (dendritic), and size-related functionalities that vary in their affinity for water (hydrophobic/hydrophilic) have all been investigated.

Mixed Functionality Rhomboids. The self-assembly of mixed crown ether and ferrocene functionalized rhomboids (Scheme 1A) was undertaken first. It is important to reiterate that the distal location of the **DB24C8** and ferrocenyl functionalities and the rigidity of the 120° donor backbone ensure that the functional groups cannot interfere directly with their respective coordination sites. It is equally important to note that the experimental conditions of each self-assembly were kept the same as in the original reports of their self-assembly[22,23] and no "external effectors" were added to the mixture in hopes of amplifying the formation of one species over another. In this way, the only means for self-organization to occur is through second-order effects resulting from the presence of the functional groups. With the knowledge from previous studies[22,23] that quantitative self-assembly does occur in each individual functionalized system, four outcomes may be expected upon mixing **DB24C8** donor **1**, ferrocenyl donor **2**, and 60° di-Pt(II) acceptor **6** in a 1:1:2 ratio: (1) exclusive heteromeric formation of mixed rhomboids containing one **DB24C8** and one ferrocenyl moiety ("social" self-organization); (2) exclusive homomeric formation of discrete bis**DB24C8** and bisferrocenyl rhomboids ("narcissistic" self-organization); (3) a purely statistical mixture of heteromeric and homomeric rhomboids (orthogonal self-assembly of individual components); (4) a mixture possessing either slightly more heteromeric or homomeric rhomboids (self-amplified organization). Scheme 2 displays a generic representation of all four possible outcomes.

One equivalent each of **DB24C8** donor **1** and ferrocenyl donor **2** were added to 2.0 equiv of di-Pt(II) acceptor **6** in 2:1 CD_3COCD_3/D_2O, and the solution was heated at 55 °C for 18 h. The homogeneous clear orange solution was then cooled to room temperature, and the composition of this complex mixture was then examined by both ^1H and $^{31}P\{1H\}$ NMR spectroscopy, as well as high-resolution electrospray ionization mass spectrometry (ESI-MS).

The ^1H NMR spectrum for the **DB24C8**/ferrocenyl mixture showed the formation of a highly symmetric species as indicated by the presence of sharp proton signals (Figure 2A). It is not possible, however, to determine the relative ratios of heteromeric and homomeric rhomboids by integration because no noticeable shifts of proton signals associated with homomeric **DB24C8** rhomboids or homomeric ferrocenyl rhomboids occur upon formation of heteromeric **DB24C8**−ferrocenyl rhomboids. The ^{31}P NMR spectrum (Figure 2B) displayed a single sharp peak at 15.5 ppm that is also indicative of the formation of discrete heteromeric or homomeric species as opposed to the formation of any oligomeric assemblies. Previous self-assembly of purely homotopic **DB24C8** and ferrocenyl rhomboids indicate that the ^{31}P NMR signals associated with the formation of their rhomboids appear at 12.6 and 12.2 ppm, respectively.[22,23,26] The appearance of one single peak in the ^{31}P NMR of the mixed **DB24C8**−ferrocenyl assembly implies that either (1) only heterotopic mixed rhomboids are formed ("social" self-organization) or (2) the ^{31}P signals associated with individual **DB24C8** and ferrocenyl rhomboids occur at the same chemical shift and it is not possible to determine whether narcissistic, social, or statistical organization is occurring.

ESI-MS, on the other hand, allows for facile resolution of peaks corresponding to individual bis**DB24C8**, bisferrocenyl, and **DB24C8**/ferrocenyl rhomboids, because there is significant variation in the molecular weight of their nitrate salts (3839.69, 3591.20, and 3342.71 g/mol, respectively). The full ESI mass spectrum is displayed in Figure 3. It is clearly evident from these ESI-MS results that $[M - 2NO_3]^{2+}$ peaks, where M represents the fully intact supramolecular assembly, associated with homomeric **DB24C8**, homomeric ferrocenyl, and heteromeric **DB24C8**−ferrocenyl rhomboids were all observed (*m*/*z* 1857.5, 1609.4, and 1733.4, respectively), and their isotopic distributions agree with theory (see Supporting Information), indicating that interpretation 2 of the ^{31}P NMR spectroscopic results is true and that all three assemblies are formed. It is interesting to note that the relative intensities of ESI-MS peaks associated with homotopic rhomboid assemblies are larger than the peak corresponding to the heterotopic, mixed assembly. While the intensities of mass spectral peaks are often not quantitative, this result is suggestive that some form of second-order self-organization may be favoring the formation of homotopic rhomboids

(26) In the original reports of the self-assembly of **DB24C8** and ferrocene functionalized rhomboids their ^{31}P NMR spectra were recorded after evaporating to dryness and re-dissolving in CD_2Cl_2, whereas in the current study, their spectra were obtained in a mixture of 2:1 CD_3COCD_3/D_2O. The different solvents account for the difference in their ^{31}P NMR chemical shifts: 12.6 and 12.2 ppm in CD_2Cl_2 (original studies) and 15.5 in CD_3COCD_3/D_2O (current study).

Scheme 2. Schematic Representation of the Four General Types of Self-Organization That Are Possible When Two Ditopic Bispyridyl Donors Are Combined with a Di-Pt(II) Acceptor in a 1:1:2 Ratio[a]

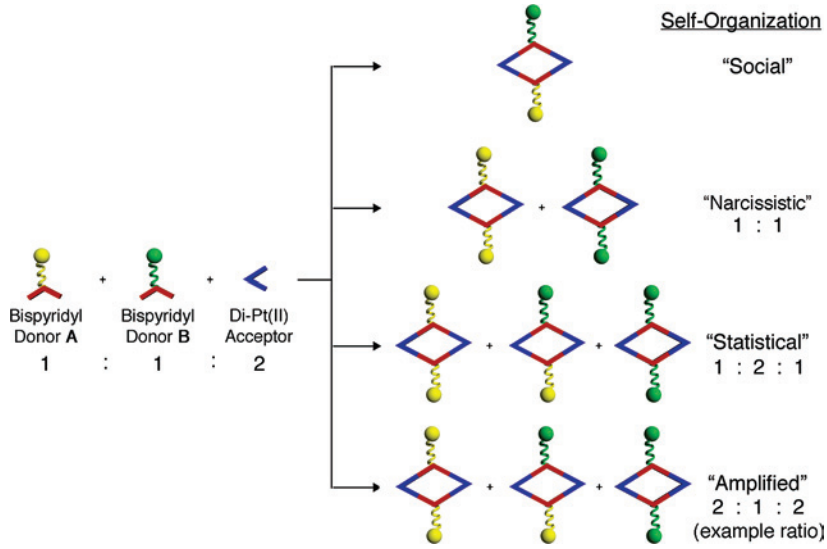

[a] "Social" is defined as exclusive formation of heterotopic metallacycles, "narcissistic" as exclusive formation of only homotopic metallacycles, "statistical" as formation of homotopic and heterotopic assemblies, and "amplified" as formation of slightly more homotopic than heterotopic metallacycles or vice versa (the ratio of 2:1:2 is only one representative example of such self-organization).

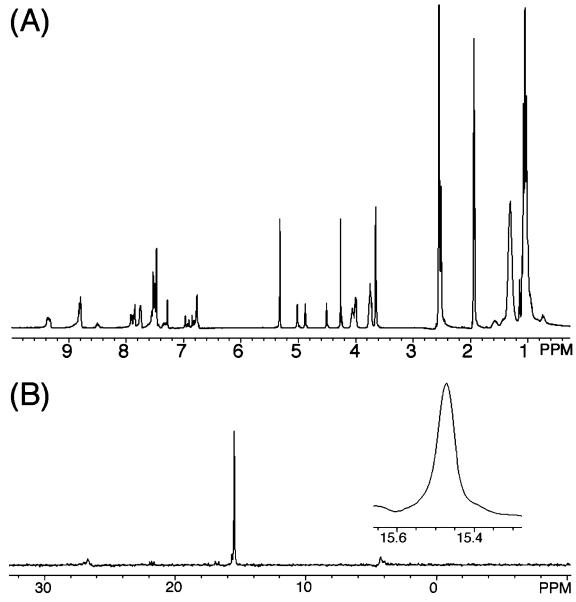

Figure 2. (A) Full ^{1}H NMR spectrum of the **DB24C8**/ferrocene mixed rhomboid self-assembly and (B) full ^{31}P NMR spectrum of the mixed assembly wherein a single, sharp ^{31}P signal (inset) indicates the formation of discrete supramolecular products.

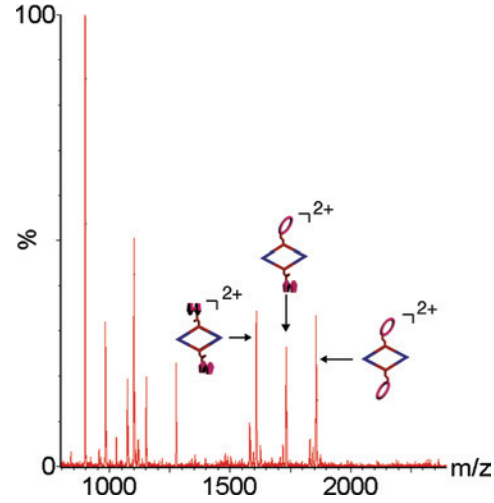

Figure 3. Full ESI mass spectrum of the complex mixture of **DB24C8** and ferrocene functionalized supramolecular rhomboids The ESI-MS results show the presence of both homotopic and heterotopic assemblies and are suggestive of the preferred formation of homotopic species.

(bis**DB24C8** and bisferrocenyl) rather than heterotopic assemblies (**DB24C8**−ferrocenyl). It remains difficult, however, to conclusively state this preference for amplified self-organization without corroborative evidence from NMR studies or other analytical techniques. The potential observation of second-order amplified self-organization is surprising given that the structural, physical, and electronic properties of the **DB24C8** and ferrocenyl functionalities are, to the best of our knowledge, unrelated and noninteracting.

Dendritic 120° bispyridyl donors **3a**−**c** share much greater structural similarity than dissimilar **DB24C8** and ferrocenyl donors **1** and **2** in that they differ only in the generation of the attached dendritic wedge. As representative examples of the complex self-assembly of mixed dendronized assemblies, we have chosen to focus on mixtures of the [G1]/[G2] (**3b** and **3c**) and [G2]/[G3] donors (**3c** and **3d**) (Scheme 1B). It is hypothesized that those donors with the largest dendritic wedges may have the greatest possibility to direct self-organization phenomena given the greater number of intermolecular dendron−dendron interactions.

Dendrons **3a** and **3b** were mixed with 60° di-Pt(II) acceptor **6** in a 1:1:2 ratio and stirred at room temperature in CD_2Cl_2 for 18 h. The same conditions were used for the mixed self-assembly of dendrons **3b** and **3c** with acceptor **6**. Each case yielded clear, homogeneous solutions that were both analyzed by multinuclear NMR spectroscopies (^{1}H and ^{31}P {^{1}H}) and ESI-MS. The [G1]/[G2] (**3a**/**3b**) and [G2]/[G3] (**3b**/**3c**) assemblies displayed sharp signals in both their ^{1}H (see Supporting Information) and ^{31}P NMR spectra

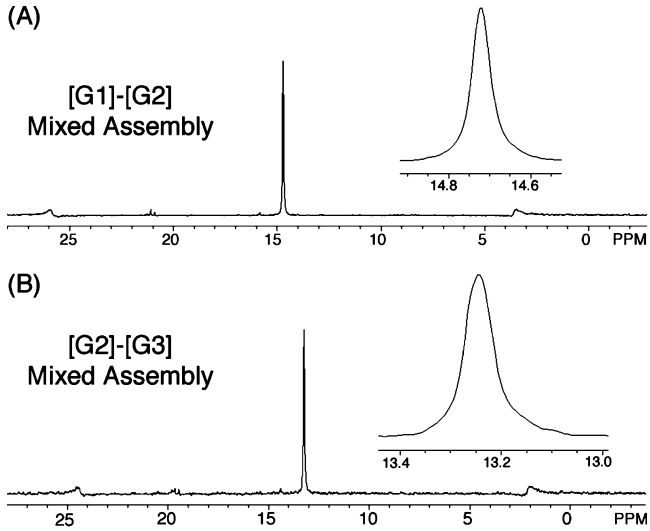

Figure 4. ^{31}P NMR spectra of (A) the [G1]/[G2] mixed dendron rhomboid assemblies and (B) the [G2]/[G3] mixed dendron rhomboid assemblies. Both spectra indicate that only discrete supramolecular species and no oligomeric species are obtained; however, differences between homotopic and heterotopic assemblies cannot be resolved.

Table 1. Observed and Calculated $[M - 2NO_3]^{2+}$ and $[M - 3NO_3]^{3+}$ Peaks (*m*/*z*) for the [G1]/[G2] and the [G2]/[G3] Mixed Dendronized Rhomboids Indicating That Both Homotopic and Mixed Heterotopic Assemblies Are Obtained

	$[M - 2NO_3]^{2+}$		$[M - 3NO_3]^{3+}$	
rhomboid	found	calculated	found	calculated
[G1]/[G2] Mixed Assembly				
[G1]−[G1]	1698.9	1699.6	1111.6	1112.4
[G1]−[G2]	1911.7	1911.2	1253.6	1253.4
[G2]−[G2]	2124.2	2124.7	1395.6	1395.8
[G2]/[G3] Mixed Assembly				
[G2]−[G2]	2124.4	2124.7	1394.9	1395.8
[G2]−[G3]	2548.0	2547.9	1678.0	1677.9
[G3]−[G3]	2971.7	2972.2	1960.9	1961.3

(Figure 4), indicating the formation of discrete supramolecular species. However, the lack of observable shifts of proton signals in the ^{1}H NMR spectra of both mixtures precluded quantitative determination of the ratios of homomeric and heteromeric products formed upon self-assembly, as did significant overlap of signals in the ^{31}P NMR spectra.

For both the [G1]/[G2] and the [G2]/[G3] mixed assemblies their ESI-MS results show the formation of heteromeric as well as homomeric rhomboid products (see Table 1). The full ESI-MS spectrum of the [G1]/[G2] mixture is shown in Figure 5A and that of the [G2]/[G3] spectrum is shown in Figure 5B. The high-resolution experimental results of each peak match their theoretical distribution (see Supporting Information) confirming the [2 + 2] molecularity of each rhomboid. As stated previously, an orthogonal self-assembly wherein there is no self-organization would lead to a statistical distribution of homomeric and heteromeric assemblies, with the heteromeric assemblies formed in a 2:1 ratio over both homomeric assemblies. While ESI-MS results cannot be evaluated quantitatively, the relative intensities of peaks in the full spectrum of the [G1]/[G2] mixture do suggest a nearly statistical distribution of homomeric and heteromeric assemblies. Figure 5A shows, for example, that the intensity of [G1]−[G2] heteromeric $[M - 2NO_3]^{2+}$ and $[M - 3NO_3]^{3+}$ peaks is greater than the intensity of the $[M - 2NO_3]^{2+}$ and $[M - 3NO_3]^{3+}$ peaks of either homodendritic ([G1]−[G1] or [G2]−[G2]) assembly. However, it can also be seen that peaks corresponding to the larger [G2]−[G2] rhomboids are less intense than those of the [G1]−[G1] assemblies. It has been observed previously that larger dendritic metallacycles are less stable under the experimental ionization conditions than smaller metallacycles,[24b] which likely explains this relative difference in intensities. Similar results are observed for the $[M - 3NO_3]^{3+}$ peaks of the [G2]/[G3] mixture (Figure 5B), which are also suggestive of a roughly statistical distribution. However, the trend in intensities of the $[M - 2NO_3]^{2+}$ peaks of the [G2]/[G3] mixture are not supportive of a statistical ratio of homomeric and heteromeric assemblies. This discrepancy is most likely due to the relative instabilities of the [G3]−[G3] and [G2]−[G3] rhomboids, the largest of those investigated, under mass conditions. All together, the collective ESI-MS results show that both homomeric and heteromeric metallacyclic rhomboids are self-assembled in both the [G1]/[G2] and [G2]/[G3] complex mixtures and are suggestive, though not conclusive, that their ratios are near-statistical.

Mixed Functionality Rectangles. The potential for self-organization of hydrophobic/hydrophilic/amphiphilic rectangles was also investigated (Scheme 1C). As before, all experimental conditions were kept constant for each self-assembly. In the case of hydrophobic and hydrophilic 180° donors, however, the additional variable of chain length could be investigated. It is important to reiterate that the overall size, shape, geometry, and binding constant of the rigid ditopic bipyridyl moieties are kept constant, as is the di-Pt(II) molecular clip (**7**). Pairs of similar length hydrophobic and hydrophilic donors, C_6/DEG, C_{12}/TEG, and C_{18}/HEG, were combined in a 1:1:2 ratio with molecular clip **7**. Again, purely amphiphilic (social self-organization), discrete hydrophobic and hydrophilic (narcissistic self-organization), statistical (orthogonal), and nonstatistical (amplified) mixtures of rectangles could be expected.

Each hydrophobic/hydrophilic pair of donors was added to the molecular clip in a 1:1:2 ratio and heated at 55 °C in CD_3COCD_3/D_2O (1.2:1) for 18 h. Upon cooling and exchange of the nitrate counterions with hexafluorophosphate (PF_6^-) anions, the mixtures were analyzed by ^{1}H and ^{31}P NMR spectroscopy and ESI-MS. The ^{1}H NMR for each mixture showed sharp peaks indicating the formation of highly symmetric species (see Supporting Information). As with the complex rhomboid mixtures, however, integration of specific peaks cannot be used to provide details of relative ratios of species in the mixtures on account of negligible shifts of proton signals associated with homomeric and heteromeric rectangles. By contrast, ^{31}P NMR spectra revealed that peaks corresponding to heteromeric (amphiphilic) rectangles appear at slightly different chemical shifts than their homomeric (hydrophobic and hydrophilic) counterparts (Figure 6).

The ^{31}P NMR spectrum for the C_6/DEG mixture, for example, showed three distinct peaks at 8.60, 8.56, and 8.53 ppm, corresponding to hydrophobic, amphiphilic, and hy-

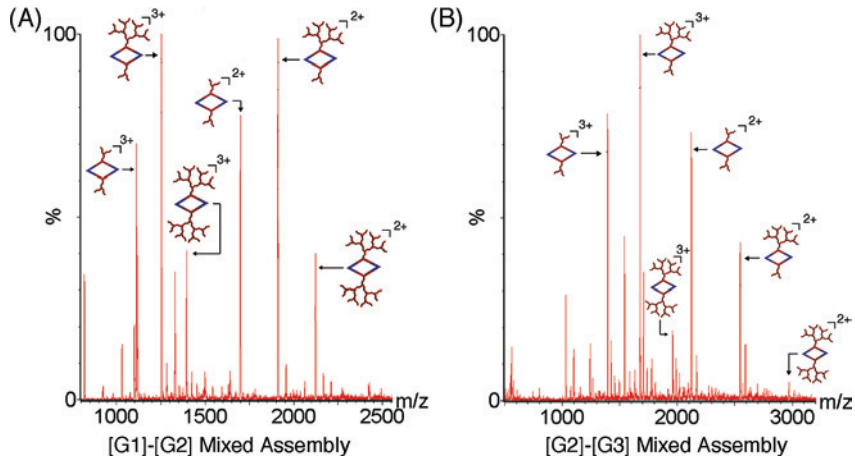

Figure 5. Full ESI mass spectra of (A) the [G1]/[G2] and (B) the [G2]/[G3] mixed assemblies. The different intensities of mass spectral peaks are suggestive of a statistical mixture of homotopic and heterotopic assemblies.

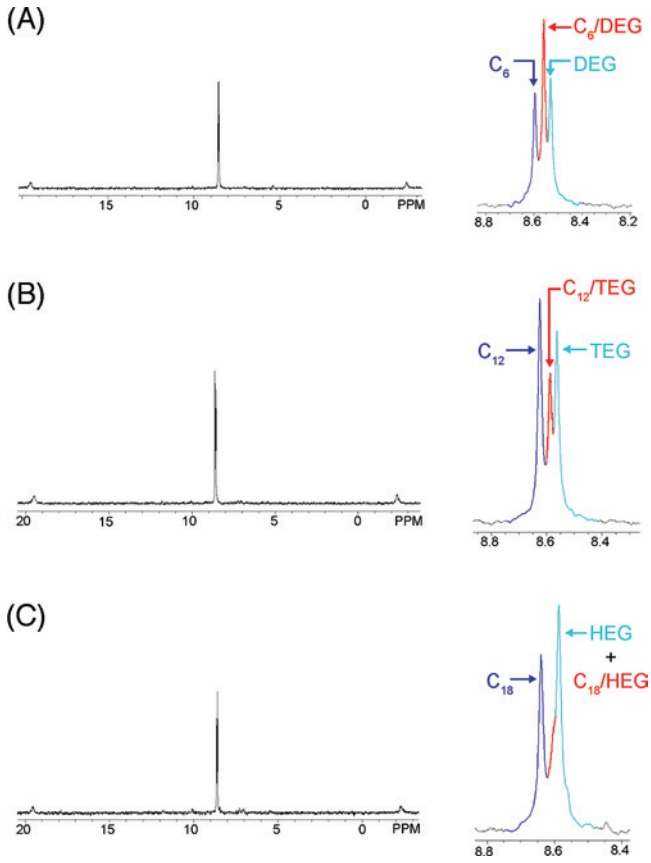

Figure 6. Full spectra and close-up views of the ^{31}P NMR spectra of the C_6/DEG (A), C_{12}/TEG (B), and C_{18}/HEG (C) mixtures showing the relative contributions of purely hydrophobic (dark blue), purely hydrophilic (light blue), and mixed amphiphilic (red) metallacycle rectangles.

drophilic rectangles, respectively (Figure 6A). Though integration of ^{31}P NMR is not as quantitative as integration of ^{1}H NMR signals, integration values of 1.0, 1.6, and 1.0 do suggest a nearly statistical mixture of rectangles with a slight deviation toward narcissistic self-organization. In the ESI-MS of the C_6/DEG mixture, peaks at m/z = 1664.4, 1682.4, and 1700.4 in agreement with the $[M - 2PF_6]^{2+}$ peaks of the hydrophilic, amphiphilic, and hydrophilic rectangles, respectively, were found and their isotopic distributions are in agreement with theory. It is interesting to note the difference in intensity of these peaks when viewed

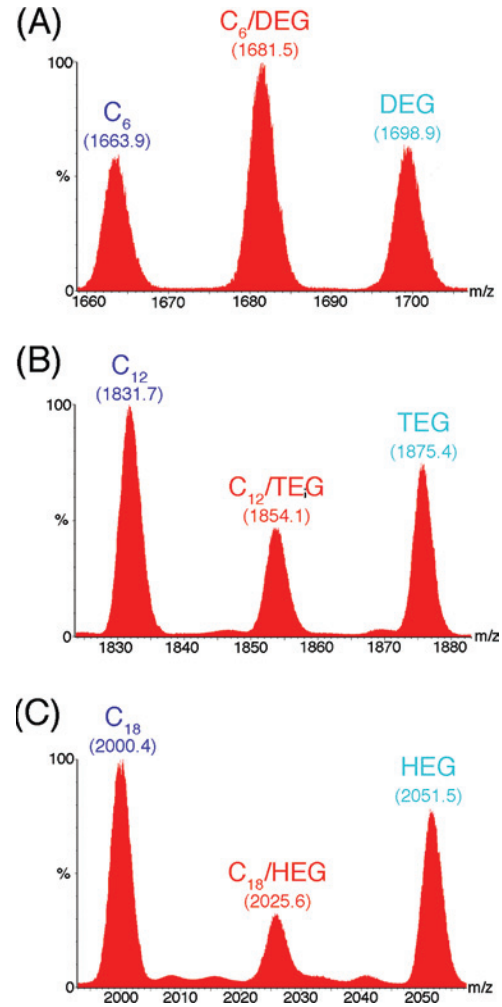

Figure 7. ESI-MS results for the C_6/DEG (A), C_{12}/TEG (B), and C_{18}/HEG (C) mixtures. The series of spectra show that with an increase in hydrophobic/hydrophilic chain length comes a decline in the presence of mixed functionality rectangles.

at the same scale (Figure 7A): the amphiphilic rectangle dominates over the two homomeric rectangles, in line with a roughly statistical distribution. These collective results strongly suggest that a near-statistical mixture is obtained from the combination of bispyridyl donors functionalized with the shortest hydrophobic and hydrophilic chains.

Examination of the ^{31}P NMR and ESI-MS spectral results for the C_{12}/TEG mixture revealed somewhat different results from those of the C_6/DEG mixture. It is immediately clear from the relative heights of phosphorus signals of the ^{31}P NMR spectrum (Figure 6B) that with these slightly longer hydrophobic and hydrophilic chains there is an amplification of homomeric species ($C_{12}-C_{12}$ at 8.63 ppm and TEG−TEG at 8.57 ppm) relative to the heteromeric amphiphilic rectangle ($C_{12}-$TEG at 8.59 ppm). Integration of signals corresponding to hydrophobic, amphiphilic, and hydrophilic species revealed an approximate ratio of 1.1:0.7:1.0. This ratio indicates a respective increase of 12% and 9% in narcissistic hydrophobic and hydrophilic self-organization and concomitant 19% decrease in the amount of social self-organization. Peaks associated with each type of rectangle were observed (Figure 7B) in the ESI-MS: m/z = 1832.7, 1854.5, and 1876.6 g/mol were found, consistent with the $[M - 2PF_6]^{2+}$ peaks of the hydrophobic, amphiphilic, and hydrophilic rectangles, respectively. Again, the isotopically resolved peaks match their theoretical distributions. When viewed together, it is apparent that the intensity of the central heteromeric peak is very nearly the same as for the two homomeric rectangles flanking it. While not quantitative, this observation supports an amplification of homomeric rectangles and provides further evidence of some extent of self-organization in the C_{12}/TEG mixture.

The trend of increased self-organization with increased chain length is continued in the C_{18}/HEG mixture. In the ^{31}P NMR spectrum (Figure 6C) of these longest hydrophobic and hydrophilic functionalized rectangles, it is clear that there is considerable, though still not pure, narcissistic self-organization. Only two phosphorus signals are visible in the spectrum, though there appears to be a slight shoulder on the signal associated with the homomeric hydrophobic rectangle, likely indicative of an unresolved signal for the amphiphilic rectangle. Integration of the two signals gives values of 1.0 and 1.4. Assuming that the relative amounts of homomeric hydrophobic and hydrophilic rectangles is roughly equal and that the difference between integration values of the signals at 8.64 ppm (purely hydrophobic) and 8.59 ppm (purely hydrophilic along with some amphiphilic) is equal to the amount of amphiphilic rectangle in the mixture, then the relative ratio of hydrophobic, amphiphilic, and hydrophilic rectangles is approximated as 1.0:0.4:1.0. Further investigation of the C_{18}/HEG mixture using ESI-MS showed peaks corresponding to the loss of two PF_6^- counterions ($[M - 2PF_6]^{2+}$) for the hydrophobic, amphiphilic, and hydrophilic rectangles at m/z = 2000.7, 2026.4, and 2052.5 g/mol, respectively (Figure 7C). When viewed at the same intensity scale, the central peak of the amphiphilic rectangle is now very near the baseline, while the flanking homomeric rectangles are significantly larger. It is therefore believed that a considerable amount of narcissistic self-organization takes place during the self-assembly of supramolecular rectangles from a complex mixture of **4c**, **5c**, and **7**.

The trend of increasing self-organization from a roughly statistical mixture (the C_6/DEG mixture) to a highly amplified homomeric mixture (the C_{18}/HEG mixture) is interesting because the functionality that determines this tendency toward self-organization is far removed from those factors that govern the self-assembly of the underlying rectangles. As opposed to variations in reaction conditions, binding interactions, or the size, shape, or geometry of constituent building blocks, the observed range of self-organization results purely from second-order effects. The results, however, can be explained in terms of a "pre-assembly" organization phenomenon that biases the resulting self-assembly of supramolecular rectangles. It is well-known and well-established in both natural and synthetic systems that molecules possessing long hydrophobic or hydrophilic chains readily aggregate into structures such as spheres, micelles, vesicles, etc.[27] Such hydrophobic/hydrophilic self-aggregation is largely dependent upon the length of the chains, with longer chains aggregating more readily, and also upon solvent wherein the aggregation of hydrophobic molecules is more facile in polar solvents (especially water) and aggregation of hydrophilic molecules is more prevalent in nonpolar solvents. While solvent has not been investigated as a variable in the studies presented here,[28] chain length has.

The relative ratios of hydrophobic, amphiphilic, and hydrophilic rectangles change from 1.0:1.6:1.0 to 1.0:0.4:1.0 in going from mixtures containing donors with the shortest (C_6/DEG) to the longest (C_{18}/HEG) hydrophobic and hydrophilic functionalities. The trend toward self-organization arises because the longer chains likely undergo a self-organization phenomenon prior to the introduction of the di-Pt(II) molecular clip, with hydrophobic donors and hydrophilic donors forming separate aggregates at thermodynamic equilibrium. When the di-Pt(II) acceptor is then added to the system, it is more likely to encounter aggregates of hydrophobic or hydrophilic donors rather than a continuous, completely randomized mixture of different donors (Scheme 3). In other words, it is more likely that di-Pt(II) acceptors will undergo self-assembly with donors of like philicity, resulting in a less than statistical mixture of supramolecular rectangle products. The Pt−N coordinative bond is, however, dynamic, and it is unlikely that donors of different philicity are exclusively segregated in solution, giving rise to some amounts of heteromeric rectangles even in the case of the C_{18}/HEG mixture. The drive toward preorganized aggregation is less strong for the shortest chains, leading to a near-statistical mixture of heteromeric and homomeric rectangles.

As a means of testing this hypothesis, two additional complex mixtures were prepared. The first was a combination of the C_6 and C_{18} donors **4a** and **4c** with molecular clip **7** in a 1:1:2 ratio, while the other was a mixture of the DEG and

(27) See, for example: (a) Jones, M. N.; Champan, D. *Micelles, Monolayers and Biomembranes*; Wiley-Liss: New York, 1995. (b) Discler, D. E.; Eisenberg, A. *Science* **2002**, *297*, 967. (c) Xia, Y.; Yang, P.; Sun, Y.; Wu, Y.; Mayers, B.; Gates, B.; Yin, Y.; Kim, F.; Han, H. *Adv. Matter.* **2003**, *15*, 353. (d) Xia, Y.; Gates, B.; Yin, Y. D.; Lu, Y. *Adv. Matter.* **2000**, *12*, 693.

(28) Previous investigations of the self-assembly of hydrophobic and hydrophilic rectangles (see ref 25) have shown that the mixture of CD_3COCD_3/D_2O used in this study is optimal for achieving quantitative self-assembly of rectangular metallacycles; therefore we chose not to vary the solvent in the current study.

Scheme 3. Schematic Representation of the Pre-assembly Aggregation Phenomena That Likely Explains the Trend toward Greater Self-Organization upon Increasing Chain Length in Mixtures of Hydrophobic (Dark Blue) and Hydrophilic (Light Blue) Bispyridyl Donors and a Di-Pt(II) Acceptor

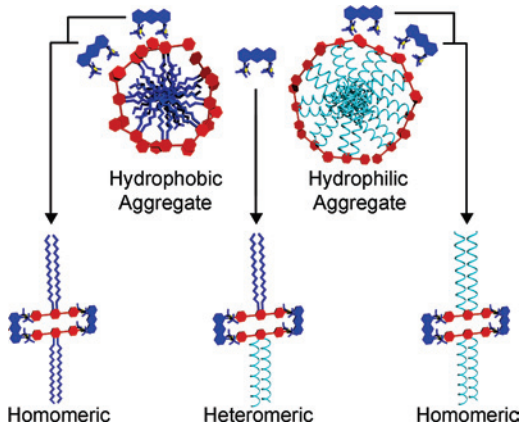

HEG donors **5a** and **5c** with molecular clip **7**, also in a 1:1:2 ratio. Assuming that any enthalpic gain from aggregation of long chain (C_{18} or HEG) donors in their respective mixtures will be outweighed by the entropic gain of a more randomized mixture, there should be little to no donor preorganization and a more statistical mixture of supramolecular rectangles should be obtained. Indeed, the ^{31}P NMR spectra of the C_6/C_{18} and DEG/HEG mixtures revealed three phosphorous signals each (Figure 8). In the case of the hydrophobic C_6/C_{18} mixture, the middle heteromeric C_6-C_{18} signal at 8.60 ppm is of roughly the same intensity of as the homomeric peaks (C_6-C_6 and $C_{18}-C_{18}$ at 8.62 and 8.59 ppm, respectively), while the ^{31}P NMR spectrum of the hydrophilic DEG/HEG mixture reveals a heteromeric DEG−HEG peak at 8.56 ppm that is of notably greater intensity that homomeric DEG−DEG and HEG−HEG peaks at 8.58 and 8.54 ppm, respectively. The increased similarity of homomeric and heteromeric rectangles in these two mixtures, however,

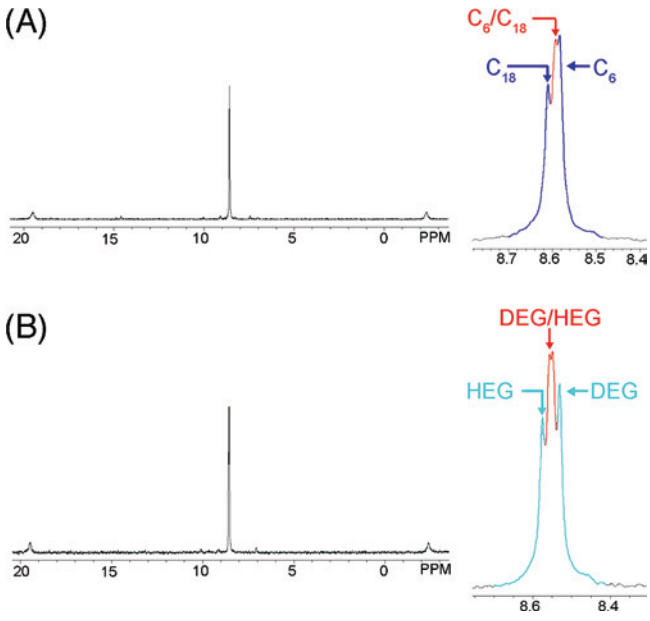

Figure 8. Full spectrum and close-up views of the ^{31}P NMR spectra of the purely hydrophobic C_6/C_{18} mixture (A) and purely hydrophilic DEG/HEG mixture (B).

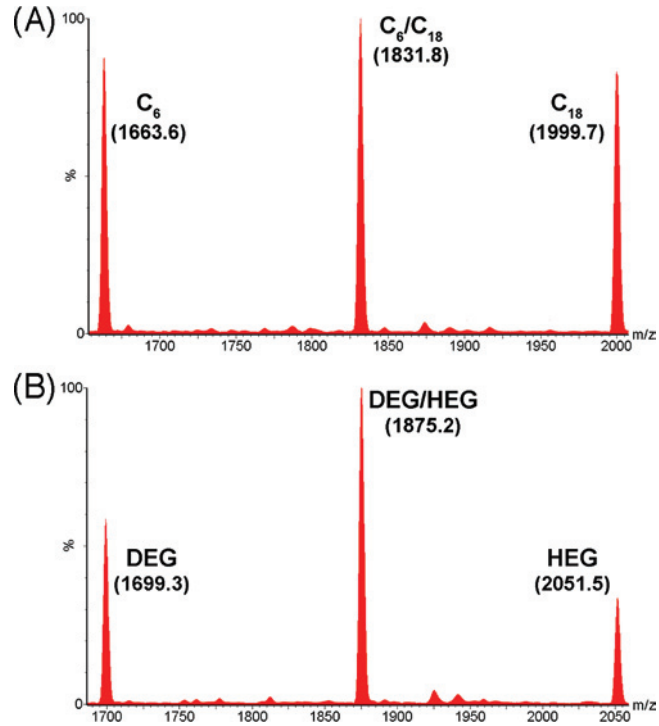

Figure 9. ESI-MS results for the hydrophobic C_6/C_{18} mixture (A) and hydrophilic DEG/HEG mixture (B).

results in an increase in signal overlap prohibiting integration of the ^{31}P NMR spectra.

ESI-MS analysis of the mixtures also revealed peaks associated with homomeric and heteromeric rectangles for each complex mixture. The $[M - 2PF_6]^{2+}$ peaks of the hydrophobic C_6, C_6/C_{18}, and C_{18} rectangles were observed at m/z = 1664.4, 1832.6, and 2000.8 g/mol, respectively, and the hydrophilic DEG, DEG/HEG, and HEG rectangles at m/z = 1700.5, 1876.6, and 2052.7 g/mol, respectively. It should be noted, however, that when viewed on the same scale (Figure 9), the intensity of the heteromeric peak for the hydrophobic C_6/C_{18} mixture is only slightly above those of the mixtures homomeric peaks, indicative of a greater than statistical amount of homomeric rectangles. This is not the case with the hydrophilic DEG/HEG mixture, where peak intensities suggest a more statistical distribution. It is likely that the high concentration of D_2O present during self-assembly results in some amounts of preorganized aggregation of hydrophobic donors in the hydrophobic mixture while disfavoring aggregation of the hydrophilic donors. Such a situation would be consistent with the slightly nonstatistical distribution of rectangles in the C_6/C_{18} mixture and essentially statistical distribution of rectangles in the DEG/HEG mixture.

Conclusion

Herein we have explored the limits of self-organization through the controlled self-assembly of a collection of supramolecular rhomboids and rectangles within complex mixtures of di-Pt(II) acceptors and bispyridyl donors containing various crown ether, ferrocenyl, dendritic, and hydrophobic/hydrophilic functionalities. The functional groups were all spatially and electronically isolated from the pyridyl moieties of the donor molecules. By keeping constant the reaction

conditions (i.e., temperature, concentration, and reaction time) and structural and thermodynamic variables (i.e., size, geometry, k_{eq}, and oxidation state and coordination geometry of the metal) of underlying molecular acceptors and donors, we could investigate the extent to which second-order interactions are able to influence, if at all, self-organization during self-assembly. In this manner, the second-order effects of seemingly unrelated (crown ether/ferrocene), structurally related though differently sized (dendritic), and size-related though different affinity for water (hydrophobic/hydrophilic) functionalities were studied. Collective NMR spectroscopic and ESI-MS results of the different complex mixtures suggest that while the mixed dendrimer assemblies do not undergo observable second-order self-organization, the hydrophobic/hydrophilic complex mixtures do show evidence of self-organization as a function of chain length, and the crown ether/ferrocene assemblies may, surprisingly, undergo some amplified self-organization. In the case of the mixed phobicity metallacyclic rectangles, the self-organization phenomena, which is supported by both NMR and ESI-MS results, can be attributed to a pre-assembly aggregation of like donors.

These studies reveal, similar to previous investigations of self-organization phenomena where reaction conditions or structural parameters were varied, that there exists a spectrum from statistical mixtures to purely narcissistic self-organization along which every complex mixture ultimately falls. While it may not always be possible to predict where a particular mixture will appear on that spectrum, it is important to investigate the wide range of potential variables that may influence self-organization in an effort to better understand which ones direct such processes more strongly than others. The discovery that second-order interactions can play a role in self-organized self-assembly reveals that control over organization does not rest solely on, in this case, the reaction conditions or nature of the donor−acceptor interaction. It is likely that similar results may be obtained for investigations of self-assembly involving hydrogen bonding, solvophobic, π-donor and π-acceptor, and other noncovalent interactions. Being able to better understand and control self-organized self-assembly is important not only for the bottom-up development of molecular materials but also for our understanding of biological systems.

In this regard, labeling the effects described herein as "second-order" may be somewhat of a misnomer: it almost goes without saying that complex functional biological systems take advantage of every potential director of self-organization whether they be proximal to primary binding sites or distal to them. Enzyme−substrate interactions, drug molecules, membranes, etc., all take advantage of the different interactions present within their structures, and their assembly and function are not solely dictated by a single interaction phenomena. While considerable progress has been made in designing synthetic analogues of biological systems, it is important to continue to explore the wide variety of means by which such abiological molecules can be induced to interact, self-assemble, and ultimately function.

Experimental Procedures

DB24C8 functionalized donor **1**,[22a] ferrocene functionalized donor **2**,[23a] dendronized donors **3a**−**c**,[24a] hydrophobic donors **4a**−**c**,[25] hydrophilic donors **5a**−**c**,[25] 60° acceptor **6**,[29] and 0° molecular clip **7**[30] were synthesized according to published literature procedures. Isolated yields of the mixed metallacycle products are given as percents by mass. Integration values for ^{1}H NMR spectral results for each mixed metallacycle system are normalized to a donor-A/donor-B/acceptor ratio of 3:3:6.

Mixed DB24C8−Ferrocene Rhomboid. Acceptor **6** (4.51 mg, 3.8 μmol) was added to a 2-dram vial. **DB24C8** functionalized donor **1** (1.46 mg, 1.9 μmol) and ferrocene functionalized donor **2** (0.99 mg, 1.9 μmol) were added to a separate glass vial, dissolved in 0.5 mL of a CD_3COCD_3/CD_2Cl_2 (1:1 v/v) solution, and transferred to the vial containing acceptor **6**. The donor vial was then washed with 3 × 0.2 mL of the mixed solvent system to ensure quantitative transfer to the vial containing acceptor **6**. The resulting suspension was stirred at room temperature for 18 h, yielding a homogeneous, clear solution. The sample was then dried under a stream of N_2(g). Yield 6.3 mg (pale orange solid), 93%. ^{1}H NMR (1:1 CD_3COCD_3/CD_2Cl_2, 300 MHz) δ 9.41−9.30 (m, 12H, H_α-Py), 8.87−8.76 (m, 24H, H_4-**6** and H_α-Py), 7.91 (d, 12H, J = 5.4 Hz, H_1-**6**), 7.86 (d, 12H, J = 5.4 Hz, H_2-**6**), 7.80−7.72 (m, 24H, H_β-Py), 7.60−7.45 (m, 21H, H_b-**2**, H_a-**2**, H_{10}-**6**), 7.28 (s, 6H, H_b-**1**), 6.98−6.80 (m, 12H, H_a-**1**, Ar*H*-**1**), 6.85−6.72 (m, 12H, Ar*H*-**1**), 5.01 (t, 6H, J = 2.1 Hz, H_c-**2**), 4.88 (t, 6H, J = 2.1 Hz, H_d-**2**), 4.50 (s, 6H, PhOCH_2), 4.26 (s, 15H, H_e-**2**), 4.09−4.03 (m, 24H, α-CH_2-**1**), 4.02−3.97 (m, 24H, β-CH_2-**1**), 3.79−3.70 (m, 24H, γ-CH_2-**1**), 1.42−1.22 (m, 144H, PCH_2CH$_3$-**6**), 1.13−0.91 (m, 216H, PCH$_2$CH_3-**6**). ^{31}P{^{1}H} NMR (1:1 CD_3COCD_3/CD_2Cl_2, 121.4 MHz) δ 15.47 (br, $^1J_{Pt\text{-}p}$ = 1354.48 Hz). MS (ESI) calcd for $[M - 2NO_3]^{2+}$ m/z 1609.1, found 1609.4 (ferrocene−ferrocene); calcd for $[M - 2NO_3]^{2+}$ m/z 1733.5, found 1733.4 (**DB24C8**−ferrocene); calcd for $[M - 2NO_3]^{2+}$ m/z 1857.9, found 1857.5 (**DB24C8**−**DB24C8**).

General Procedure for Preparation of Mixed Dendritic Rhomboids. Acceptor **6** (2.0 equiv) was added to a 2-dram glass vial. Two different generation dendronized 120° donors (**3a** and **3b** or **3b** and **3c**, 1.0 equiv each) were then added to a separate glass vial, dissolved in CD_2Cl_2 (0.5 mL), and transferred to the vial containing acceptor **6**. Quantitative transfer was ensured by washing the donor vial with additional CD_2Cl_2 (3 × 0.2 mL). The reaction mixture was allowed to stir at room temperature for 18 h, resulting in a clear, homogeneous solution, which was transferred directly to an NMR tube for spectroscopic analysis. Following spectroscopic analysis, the samples were dried under a stream of N_2(g) and weighed.

[G1]/[G2] Mixed Assembly. Reaction scale: acceptor **6** (4.98 mg, 4.3 μmol), donor **3a** (1.29 mg, 2.15 μmol), donor **3b** (2.18 mg, 2.15 μmol). Yield 8.1 mg (pale yellow solid), 96%. ^{1}H NMR (CD_2Cl_2, 300 MHz) δ 9.38 (d, 12H, J = 5.7 Hz, H_α-Py), 8.85 (s, 12H, H_4-**6**), 8.69 (d, 12H, J = 5.7 Hz, H_α-Py), 7.96 (d, 12H, J = 5.4 Hz, H_2-**6**), 7.78 (dd, 12H, J = 11.3, 5.4 Hz, H_1-**6**), 7.66 (s, 12H, H_{10}-**6**), 7.59 (d, 24H, J = 5.7 Hz, H_β-Py), 7.48−7.32 (m, 126H, Ph*H* and Ar*H*), 6.73 (m, 12H, H_b), 6.63−6.55 (m, 6H, H_a), 5.15 (s, 12H, OCH_2Ar), 5.08 (s, 12H, OCH_2Ph), 5.06 (s, 24H, OCH_2Ph), 5.03 (s, 12H, OCH_2Ph), 1.43−1.30 (m, 144H, PCH_2CH$_3$-**6**), 1.20−1.05 (m, 216H, PCH$_2$CH_3-**6**). ^{31}P{^{1}H} NMR (CD_2Cl_2, 121.4 MHz) δ 14.72 (br, $^1J_{Pt\text{-}p}$ = 1365.2 Hz). MS (ESI)

calcd for $[M - 2NO_3]^{2+}$ *m*/*z* 1689.9, found 1699.6 ([G1]−[G1]); calcd for $[M - 2NO_3]^{2+}$ *m*/*z* 1911.7, found 1911.2 ([G1]−[G2]); calcd for $[M - 2NO_3]^{2+}$ *m*/*z* 2124.2, found 2124.7 ([G2]−[G2]); calcd for $[M - 3NO_3]^{3+}$ *m*/*z* 1111.6, found 1112.4 ([G1]−[G1]); calcd for $[M - 3NO_3]^{3+}$ *m*/*z* 1253.6, found 1253.4 ([G1]−[G2]); calcd for $[M - 3NO_3]^{3+}$ *m*/*z* 1395.6, found 1395.8 ([G2]−[G2]).

[G2]/[G3] Mixed Assembly. Reaction scale: acceptor **6** (3.01 mg, 2.6 μmol), donor **3b** (1.33 mg, 1.3 μmol), donor **3c** (2.41 mg, 1.3 μmol). Yield 6.4 mg (pale yellow solid), 95%. ^{1}H NMR (CD_2Cl_2, 300 MHz) δ 9.37 (d, 12H, J = 6.0 Hz, H_α-Py), 8.86 (s, 12H, H_4-**6**), 8.68 (d, 12H, J = 5.8 Hz, H_α-Py), 7.95 (d, 12H, J = 5.7 Hz, H_2-**6**), 7.79−7.73 (m, 12H, H_1-**6**), 7.66 (s, 12H, H_{10}-**6**), 7.58 (d, 24H, J = 6.0 Hz, H_β-Py), 7.50−7.25 (m, 198H, Ar*H*), 6.76−6.65 (m, 60H, Ar*H* and H_b), 6.56−6.53 (m, 30H, Ar*H* and H_a), 5.14(s, 12H, OCH_2Ar), 5.08 (s, 24H, OCH_2Ph), 5.06 (s, 24H, OCH_2Ph), 5.04−4.92 (m, 84H, OCH_2Ph), 1.42−1.27 (m, 144H, PCH_2CH$_3$-**6**), 1.20−1.00 (m, 216H, PCH$_2$CH_3-**6**). ^{31}P{^{1}H} NMR (CD_2Cl_2, 121.4 MHz) δ 13.25 (br, $^1J_{Pt\text{-}p}$ = 1370.68 Hz). MS (ESI) calcd for $[M - 2NO_3]^{2+}$ *m*/*z* 2124.4, found 2124.7 ([G2]−[G2]); calcd for $[M - 2NO_3]^{2+}$ *m*/*z* 2548.0, found 2547.9 ([G2]−[G3]); calcd for $[M - 2NO_3]^{2+}$ *m*/*z* 2971.7, found 2972.2 ([G3]−[G3]); calcd for $[M - 3NO_3]^{3+}$ *m*/*z* 1394.9, found 1395.8 ([G2]−[G2]); calcd for $[M - 3NO_3]^{3+}$ *m*/*z* 1678.0, found 1677.9 ([G2]−[G3]); calcd for $[M - 3NO_3]^{3+}$ *m*/*z* 1960.9, found 1961.3 ([G3]−[G3]).

General Procedure for Preparation of Mixed Functionality Supramolecular Rectangles. One equivalent each of a hydrophobic donor (**4a**−**c**) and a hydrophilic donor (**5a**−**c**) were added to a glass vial. To another glass vial was added 2.0 equiv of 0° molecular clip **7**. The mixed donors were taken up in 0.5 mL of CD_3COCD_3/D_2O (1.2:1) and transferred to the vial containing acceptor **7**. This process was repeated (3 × 0.4 mL) to ensure quantitative transfer. The glass vial was sealed with Teflon tape and heated at 55−60 °C for 18 h, after which time a homogeneous orange solution had formed. The solution was concentrated under a stream of N_2(g), and a saturated H_2O solution of KPF_6 was added in order to exchange the NO_3^- anions to PF_6^- counterions. The product was washed several times with H_2O, and the resulting solid was collected.

C_6/DEG Mixed Assembly. Reaction scale: acceptor **7** (14.42 mg, 12.4 μmol), donor **4a** (3.0 mg, 6.2 μmol), donor **5a** (3.2 mg, 6.2 μmol). Yield 21.7 mg (orange solid), 96%. ^{1}H NMR (CD_3COCD_3, 300 MHz) δ 9.56 (s, 6H, H_9-**7**), 9.24 (dd, 12H, J = 15.9, 5.4 Hz, H_α-Py-**4a**), 9.13 (d, 12H, J = 5.5 Hz, H_α-Py-**5a**), 8.53 (s, 6H, H_{10}-**7**), 8.27 (s, 12H, H_β-Py-**5a**), 8.15 (dd, 12H, J = 15.9, 5.6 Hz, H_β-Py-**4a**), 7.89−7.78 (m, 24H, $H_{2,4,5,7}$-**7**), 7.58−7.49 (m, 12H, $H_{3,6}$-**7**), 7.32−7.22 (m, 12H, Ar*H*), 4.55−4.45 (m, 12H, H_{glycol}-**5a**), 4.31 (t, 12H, J = 6.3 Hz, ArOCH_2-**4a**), 3.98−3.91 (m, 12H, H_{glycol}-**5a**), 3.72−3.66 (m, 12H, H_{glycol}-**5a**), 3.55−3.49 (m, 12H, H_{glycol}-**5a**), 3.30 (s, 18H, -OCH_3-**5a**), 1.97−1.85 (m, 12H, H_{alkane}-**4a**), 1.79−1.50 (m, 156H, PCH_2CH$_3$-**7** and H_{alkane}-**4a**), 1.44−1.28 (m, 24H, H_{alkane}-**4a**), 1.10−0.90 (m, 236H, PCH$_2$CH_3-**7** and -CH$_3$-**4a**). ^{31}P{^{1}H} NMR (CD_3COCD_3, 121.4 MHz) δ 8.60, 8.56, 8.53 (all singlets, $^1J_{Pt\text{-}p}$ = 1330.55 Hz). MS (ESI) calcd for $[M - 2PF_6]^{2+}$ *m*/*z* 1664.6, found 1664.4 (C_6−C_6); calcd for $[M - 2PF_6]^{2+}$ *m*/*z* 1682.6, found 1682.4 (C_6−DEG); calcd for $[M - 2PF_6]^{2+}$ *m*/*z* 1700.6, found 1700.4 (DEG−DEG).

C_{12}/TEG Mixed Assembly. Reaction scale: acceptor **7** (10.7 mg, 9.2 μmol), donor **4b** (3.0 mg, 4.6 μmol), donor **5b** (3.2 mg, 4.6 μmol). Yield 17.3 mg (orange solid), 94%. ^{1}H NMR (CD_3COCD_3, 300 MHz) δ 9.55 (s, 6H, H_9-**7**), 9.29−9.19 (m, 12H, H_α-Py-**4b**), 9.13 (d, 12H, J = 5.7 Hz, H_α-Py-**5b**), 8.54 (s, 6H, H_{10}-**7**), 8.31−8.21 (m, 12H, H_β-Py-**5b**), 8.20−8.11 (m, 12H, H_β-Py-**4b**), 7.88−7.80 (m, 24H, $H_{2,4,5,7}$-**7**), 7.55−7.52 (m, 12H, $H_{3,6}$-**7**), 7.31−7.25 (m, 12H,Ar*H*), 4.54−4.49 (m, 12H, H_{glycol}-**5b**), 4.32 (t, 12H, J = 6.2 Hz, ArOCH_2-**4b**), 3.99−3.93 (m, 12H, H_{glycol}-**5b**), 3.73−3.67 (m, 12H, H_{glycol}-**5b**), 3.64−3.55 (m, 48H, H_{glycol}-**5b**), 3.49−3.44 (m, 12H, H_{glycol}-**5b**), 3.28 (s, 18H, -OCH_3-**5b**), 2.00−1.87 (m, 12H, H_{alkane}-**4b**), 1.75−1.50 (m, 156H, PCH_2CH$_3$ and H_{alkane}-**4b**), 1.41−1.22 (m, 96H, H_{alkane}-**4b**), 1.07−0.92 (m, 236H, PCH$_2$CH_3 and -CH$_3$-**4b**). ^{31}P{^{1}H} NMR (CD_3COCD_3, 121.4 MHz) δ 8.63, 8.59, 8.57 (all singlets, $^1J_{Pt\text{-}p}$ = 1324.10 Hz). MS (ESI) calcd for $[M - 2PF_6]^{2+}$ *m*/*z* 1832.8, found 1832.7 (C_{12}−C_{12}); calcd for $[M - 2PF_6]^{2+}$ *m*/*z* 1854.7, found 1854.5 (C_{12}−TEG); calcd for $[M - 2PF_6]^{2+}$ *m*/*z* 1876.7, found 1876.6 (TEG−TEG).

C_{18}/HEG Mixed Assembly. Reaction scale: acceptor **7** (8.37 mg, 7.2 μmol), donor **4c** (3.0 mg, 3.6 μmol), donor **5c** (3.1 mg, 3.6 μmol). Yield 15.0 mg (orange solid), 96%. ^{1}H NMR (CD_3COCD_3, 300 MHz) δ 9.55 (s, 6H, H_9-**7**), 9.27−9.18 (m, 12H, H_α-Py-**4c**), 9.15−9.09 (m, 12H, H_α-Py-**5c**), 8.54 (s, 6H, H_{10}-**7**), 8.31−8.18 (m, 12H, H_β-Py-**5c**), 8.14−8.05 (m, 12H, H_β-Py-**4c**), 7.88−7.80 (m, 24H, $H_{2,4,5,7}$-**7**), 7.56−7.50 (m, 12H, $H_{3,6}$-**7**), 7.30−7.24 (m, 12H, Ar*H*), 4.54−4.48 (m, 12H, H_{glycol}-**5c**), 4.32 (t, 12H, J = 6.9 Hz, ArOCH$_2$-**4c**), 3.99−3.93 (m, 12H, H_{glycol}-**5c**), 3.73−3.68 (m, 12H, H_{glycol}-**5c**), 3.65−3.51 (m, 96H, H_{glycol}-**5c**), 3.48−3.43 (m, 12H, H_{glycol}-**5c**), 3.27 (s, 18H, -OCH_3-**5c**), 2.00−1.89 (m, 12H, H_{alkane}-**4c**), 1.75−1.52 (m, 156H, PCH_2CH$_3$ and H_{alkane}-**4c**), 1.43−1.25 (m, 168H, H_{alkane}-**4c**), 1.08−0.92 (m, 236H, PCH$_2$CH_3 and -CH$_3$-**4c**). ^{31}P{^{1}H} NMR (CD_3COCD_3, 121.4 MHz) δ 8.64 (s), 8.59 (s with a broad shoulder) $^1J_{Pt\text{-}p}$ = 1325.62 Hz. MS (ESI) calcd for $[M - 2PF_6]^{2+}$ *m*/*z* 2001.0, found 2000.7 (C_{18}−C_{18}); calcd for $[M - 2PF_6]^{2+}$ *m*/*z* 2026.4, found 2026.4 (C_{18}−HEG); calcd for $[M - 2PF_6]^{2+}$ *m*/*z* 2052.8, found 2052.5 (HEG−HEG).

C_6/C_{18} Mixed Assembly. Reaction scale: acceptor **7** (19.3 mg, 16.6 μmol), donor **4a** (4.0 mg, 8.3 μmol), donor **4c** (6.8 mg, 8.3 μmol). Yield 31.8 mg (yellow solid), 97%. ^{1}H NMR (CD_3COCD_3, 300 MHz) δ 9.55 (s, 6H, H_9-**7**), 9.20 (dd, 24H, J = 36.0, 5.1 Hz, H_α-Py), 8.54 (s, 6H, H_{10}-**7**), 8.29−8.20 (m, 12H, H_β-Py), 8.13 (d, 12H, J = 5.1 Hz, H_β-Py), 7.88−7.81 (m, 24H, $H_{2,4,5,7}$-**7**), 7.53 (s, 12H, Ar*H*), 7.31−7.24 (m, 12H, $H_{3,6}$-**7**), 4.31 (t, 24H, J = 6.6 Hz, ArOCH_2), 2.00−1.85 (m, 24H, H_{alkane}), 1.75−1.51 (m, 192H, PCH_2CH$_3$ and H_{alkane}), 1.43−1.24 (m, 168H, H_{alkane}), 1.08−0.92 (m, 216H, PCH$_2$CH_3), 0.91−0.84 (m, 36H, -CH$_3$). ^{31}P{^{1}H} NMR (CD_3COCD_3, 121.4 MHz) δ 8.62, 8.60, 8.59 (all singlets, $^1J_{Pt\text{-}p}$ = 1331.27 Hz). MS (ESI) calcd for $[M - 2PF_6]^{2+}$ *m*/*z* 1664.6, found 1664.4 (C_6−C_6); calcd for $[M - 2PF_6]^{2+}$ *m*/*z* 1832.8, found 1832.6 (C_6−C_{18}); calcd for $[M - 2PF_6]^{2+}$ *m*/*z* 2001.0, found 2000.8 (C_{18}−C_{18}).

DEG/HEG Mixed Assembly. Reaction scale: acceptor **7** (13.5 mg, 11.6 μmol), donor **5a** (3.0 mg, 5.8 μmol), donor **5c** (5.0 mg, 5.8 μmol). Yield 22.2 mg (orange solid), 95%. ^{1}H NMR (CD_3COCD_3, 300 MHz) δ 9.56 (s, 6H, H_9-**7**), 9.17 (dd, 24H, J = 24.9, 5.7 Hz, H_α-Py), 8.53 (dd, 24H, J = 24.7, 5.7 Hz, H_β-Py), 7.89−7.79 (m, 24H, $H_{2,4,5,7}$-**7**), 7.53 (s, 12H, Ar*H*), 7.31−7.24 (m, 12H, $H_{3,6}$-**7**), 4.54−4.46 (m, 24H, H_{glycol}), 3.98−3.92 (m, 24H, H_{glycol}), 3.73−3.66 (m, 24H, H_{glycol}), 3.65−3.42 (m, 120H, H_{glycol}), 3.30 (s, 18H, -OCH$_3$), 3.27 (s, 18H), 1.78−1.52 (m, 144H, PCH_2CH$_3$), 1.09−0.86 (m, 216H, PCH$_2$CH_3). ^{31}P{^{1}H} NMR (CD_3COCD_3, 121.4 MHz) δ 8.58, 8.56, 8.54 (all singlets, $^1J_{Pt\text{-}p}$ = 1325.33 Hz). MS (ESI) calcd for $[M - 2PF_6]^{2+}$ *m*/*z* 1700.0, found 1700.5 (DEG−DEG); calcd for $[M - 2PF_6]^{2+}$ *m*/*z* 1876.6, found 1876.6 (DEG−HEG); calcd for $[M - 2PF_6]^{2+}$ *m*/*z* 2052.8, found 2052.7 (HEG−HEG).

Acknowledgment. P.J.S. thanks the NIH (Grant GM-057052) and the NSF (Grant CHE-0306720) for financial support. B.H.N. thanks the NIH (Grant GM-080820) for financial support.

Supporting Information Available: ^{1}H NMR spectra of mixed dendritic and rectangular assemblies, as well as high-resolution ESI-MS data for all heterotopic rhomboid and rectangular metallacycles. This material is available free of charge via the Internet at http://pubs.acs.org.

IC801711Q

(29) Kryschenko, Y. K.; Seidel, S. R.; Arif, A. M.; Stang, P. J. *J. Am. Chem. Soc.* **2003**, *125*, 5193.
(30) Kuehl, C. J.; Huang, S. D.; Stang, P. J. *J. Am. Chem. Soc.* **2001**, *123*, 9634.